Quantifying and Comparing the Intersegmental Kinematics of the Pediatric Whole Cervical Spine to Individual Motion Segment Kinematics in a Six-Year-Old PMHS

M.Liu[1] and J.F. Luck, PhD[1]
[1] Duke University

ABSTRACT

Mitigating both neck and head injuries in the pediatric population relies heavily on improving our understanding of the underlying biomechanics of the pediatric cervical spine. The tensile response for individual motion segments and the whole cervical spine (WCS) has been reported, but there is no data characterizing the intersegmental kinematics of pediatric WCS under axial loading conditions. The structural response of motion segments and WCS provide valuable data for the design and validation of biofidelic physical and computational models for the pediatric population. However, the use of motion segment data to construct WCS response or the use of WCS axial response to accurately characterize intersegmental response may present limitations to accurately modeling the pediatric cervical spine response. In this secondary analysis of the work of Luck et al. (2008 and 2013), the fixed-fixed, low load, quasi-static tensile response of the WCS and individual motion segments (O-C2, C4-C5, and C6-C7) of a six-year-old postmortem human surrogate (PMHS) was investigated to quantify and compare the intersegmental kinematics under both conditions. In the whole spine, O-C2, C3-C4, C6-C7, and C7-T1 exhibited a tensile response, C2-C3 and C5-C6 exhibited a compressive response, and C4-C5 did not exhibit an appreciable response in the axial loading direction. Furthermore, when compared to the tensile behavior of the individual motion segment load-controlled tests, C6-C7 exhibited reduced axial displacement and an increased stiffness at higher loads (≥13.5N), suggesting the recruitment of more superficial ligamentous layers that span multiple vertebrae in the whole spine. Regarding vertical displacement and rotation, O-C2 exhibited the largest amount of rotation of 5.57 degrees in flexion and all segments exhibited some amount of anterior-posterior (AP) displacement. The intersegmental kinematics provide biomechanical response data that may support both physical and computational surrogate design and validation as well as data for comparison to isolated FSU testing conditions.

INTRODUCTION

The global incidence of pediatric traumatic spinal injury (TSI) is estimated to be around 14.2 per 100,000 children with 30.6% requiring surgical intervention. Across all regions, road traffic accidents are the leading cause of injury, accounting for 46% to 74% of all pediatric TSI (Haizel-Cobbina et al., 2023). In the United States, pediatric cervical spine injury accounts for around 2% of all pediatric trauma admissions with an overall mortality rate of 4-5% (Shin et al.,

This paper is a student paper from the 19th Injury Biomechanics Symposium and is published in a special issue of SAE International Journal of Transportation Safety.
It is preliminary work, has not been peer reviewed, and should not be cited because it is a work in progress.

2016; Poorman et al., 2019). However, pediatric cervical spine injury accounts for about 80% of all pediatric spinal injuries with 80% of the cases occurring in adolescents and young adults (Shin et al., 2016). Traffic accidents have been reported to be the most frequent cause of cervical spine injury across all age groups, contributing to more than 50% of all cervical spine injuries (Shin et al., 2016; Poorman et al., 2019).

Furthermore, the cervical spine contributes to head kinematics in dynamic loading conditions and is therefore an important and relevant component for consideration in terms of head and traumatic brain injuries (TBI) and related neurological deficits (Araki et al., 2017; Leonard et al., 2019). Due to higher head to body weight ratio, weaker musculature, and lower spine stiffness, the pediatric TBI characteristics and considerations differ from that of adults (Araki et al., 2017). In the pediatric population, TBIs are the leading cause of death and disability, where 61% of moderate to severe TBI results in a disability and where medical expenditures are estimated to be $667 million per year (Shen et al., 2021; Haarbauer-Krupa et al., 2018). The most common mechanisms of pediatric TBI are falls and motor vehicle accidents (Lu et al., 2022). For children 5 years and older, sports and recreational-related injuries are also one of the common mechanisms of brain injury (Thurman, 2016).

To date, anthropomorphic test devices (ATD) and finite element models (FEM) are two of the primary ways to model the body's response under potentially injurious loading conditions and assist in developing strategies to mitigate potential injuries. Both methods provide benefits over human volunteer studies (which are limited to low load, non-injurious conditions), post-mortem human surrogates (PMHS) (which are limited by availability, lack of muscle response, and ethical considerations), and animal surrogates (which are limited by interspecies anatomical and physiological differences) (Crandell et al., 2011). However, the biofidelity of physical and computational models may rely on the level of biofidelity of the underlying components that join together to form an ATD or human-body model (Dibb et al., 2014). This emphasizes the importance of laboratory mechanical testing under various loading conditions to obtain the structural or material response data necessary for accurately characterizing tissue response.

Current pediatric neck models are designed and validated by scaling down adult models via size, anatomical, and mechanical properties and by using data from pediatric volunteer and surrogate studies. For example, the neck of the Hybrid III child ATDs were scaled down versions of the Hybrid III adult ATDs using geometric data such as total body weight and neck circumference (Irwin & Mertz, 1997). To accurately translate the measurements made using ATDs and/or computational models tests human injury risk, injury criteria and risk curves based on volunteer and surrogate studies are developed (Mertz et al., 2003). However, differences observed in the kinematics and kinetic response between ATDs to human volunteers under low load impacts have suggested that the biofidelity of the Hybrid III child ATDs might be improved (Seacrist et al., 2012; Seacrist et al., 2013).

Similar to physical models, computational models also rely on material properties and/or structural response data derived from biomechanical testing of biological tissues for defining model response, parameter tuning and validation purposes. Prior efforts in developing FE models of the pediatric cervical spine have relied on scaling down the adult cervical spine based on

This paper is a student paper from the 19th Injury Biomechanics Symposium and is published in a special issue of SAE International Journal of Transportation Safety.
It is preliminary work, has not been peer reviewed, and should not be cited because it is a work in progress.

geometric size and bone density (Dong et al., 2013; Dibb et al., 2014). In Dong et al., the tensile test results of Luck et al. (2008, 2013) were used to validate the FEM of a 10-year-old ligamentous cervical spine. On the other hand, in Dibb et al. (2011, 2014), the stiffnesses of the pediatric model's intervertebral joints were derived from Luck et al. (2008, 2013) and overall head-neck model response was validated with lower speed frontal impacts performed by Arbogast et al. (2009).

Although the osteoligamentous tensile properties (stiffness, failure load, ultimate displacement, etc.) for individual motion segments and the whole cervical spine has been reported (Luck et al., 2008; Luck et al., 2013; Ouyang et al., 2005), there is no data characterizing the intersegmental kinematics of pediatric whole spines under axial loading conditions nor are there analysis of these data that would provide greater insight into how pediatric whole spine tensile response is related to tensile response obtained from isolated individual motion segments. This study aims to quantify and compare the intersegmental kinematics of a pediatric whole cervical tensile test to corresponding individual motion segment tests to aid the design and validation of biofidelic physical and computational models for the pediatric population.

METHODS

Original Experiment

This section provides a summary of the portions of the original experiments that are relevant to this study. Further details of the original experimental methodology are provided in previous publications (Luck et al., 2008; Luck et al., 2013).

In this study investigating the tensile response of the developing pediatric cervical spine, the osteoligamentous whole cervical spine (WCS) and functional spinal units (FSU) of an unembalmed six-year-old pediatric human cadaver were investigated. The surrogate was a six-year-old female with a non-pathological cervical spine. The subject had a cervical spine length of 8.98 centimeters, and a T1 endplate width and depth of 25.40 and 13.75mm, respectively. The whole cervical spine was loaded to 10% of the estimated failure load under load control. Details of how the estimated failure load and loading rates were determined can be obtained in the prior study (Luck et al., 2008; Luck et al., 2013). The peak load for this specific specimen was calculated to be 177.6 N and the loading rate was set as 44.4 N/sec.

Prior to the WCS testing, the skin, subcutaneous fatty tissue, and neck musculature were removed to isolate the osteoligamentous spine. Furthermore, the mandible was removed to allow for rigid head/skull fixation and visualization of the upper cervical spine. The Frankfort plane was aligned to be horizontal and the head was embedded in polymethylmethacrylate (PMMA) (Dentsply International; York, PA) to ensure a rigid connection to the testing frame. The Frankfort plane was defined from the superior point of the external auditory meatus to the infraorbital foramen. Similarly, T1 was cast in PMMA and resin and secured with K-wires and pedicle loops

This paper is a student paper from the 19th Injury Biomechanics Symposium and is published in a special issue of SAE International Journal of Transportation Safety.
It is preliminary work, has not been peer reviewed, and should not be cited because it is a work in progress.

to ensure rigid connection to an aluminum cup that was rigidly attached to the linear actuator. The WCS was attached with normal lordosis and the angle measurements obtained from the high-speed video of the tests align with those reported in the literature. The measured C7 angle with the horizontal in the initial position prior to loading of 27.6 degrees in flexion was in range of the mean C7 slope (21.3 ± 6.9 degrees) reported by Abelin-Genevois et al. (2014). Furthermore, the measured O-C2 angle of -7.3 degrees was in the range of the O-C2 angle (−15.2 ±6.7 degrees) reported by Abelin-Genevois et al. (2014). Motion tracking of individual cervical vertebrae was obtained by inserting a multi-point tracking marker into the anterior face of the vertebral body of each vertebra from C2 to T1. An example of marker placement is as shown in Figure 1. Due to the low loading rate and low peak load, it is assumed that the tracking markers did not experience appreciable vibratory movements across the course of loading and are representative of the rigid body motion of the vertebrae. Furthermore, it was assumed that the two arms of the multi-point tracking marker were perpendicular to each other.

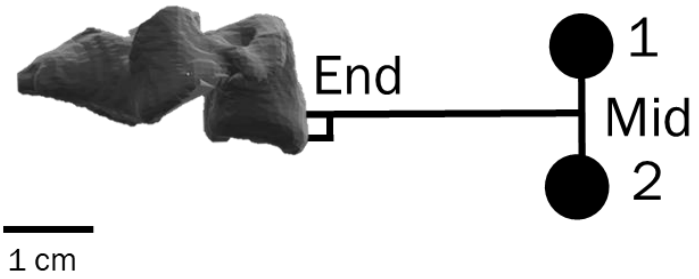

Figure 1: C3 segment (generated from CT scan of 6YO PMHS) with the T-shaped marker. It is assumed that the marker is rigidly inserted normally to the anterior face of the vertebral body. The balls on the T-shaped marker (labelled 1 and 2) were tracked and the length of each beam was obtained to calculate the rotation and translation of each vertebra. The midpoint and endpoint as labelled were then calculated.

A testing frame, as shown in Figure 2, was used for the WCS tensile tests. A six-axis load cell (2554A, Denton, Inc., Rochester Hills, MI) rigidly fixed to the top of the frame measured the loads while an LVDT (linear variable differential transformer) attached to the hydraulic actuator (227, MTS Systems Corporation, Eden Prairie, MN) measured the linear displacement of the bottom plate. The sensor data was recorded via a digital acquisition system (LabView 7.0, PCI 6071E, National Instruments, Austin, TX). Prior to the actual tensile test, the WCS was preconditioned under load control at 1 Hz for sixty seconds under fixed-fixed condition.

This paper is a student paper from the 19th Injury Biomechanics Symposium and is published in a special issue of SAE International Journal of Transportation Safety.
It is preliminary work, has not been peer reviewed, and should not be cited because it is a work in progress.

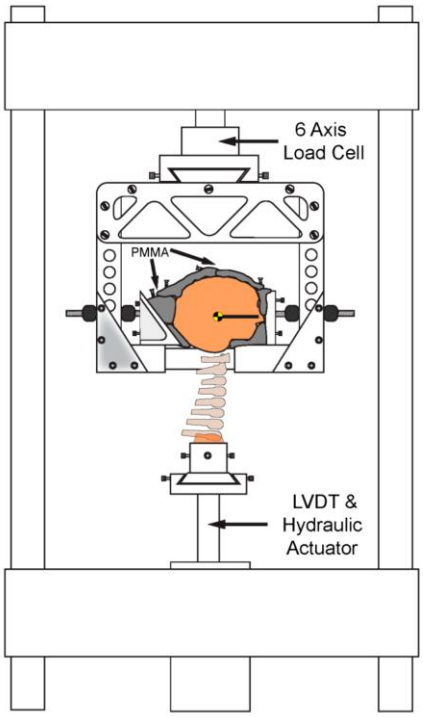

Figure 2: Pediatric whole spine tensile test setup as presented in Luck et al., 2008. The skull and the base were potted in PMMA to ensure rigid attachment to the testing setup.

After the WCS test, individual motion segments (O-C2, C4-C5, and C6-C7) were disarticulated and tested under fixed-fixed conditions with the same rate of loading (44.4 N/sec) to the same peak load of 177.6 N. The testing setup is as shown in Figure 3. During the disarticulation, intervertebral ligaments such as the anterior and posterior longitudinal ligaments (ALL and PLL) and the nuchal ligament were dissected to fully isolate each FSU. Prior to the individual motion segment tests, the segments were once again preconditioned to 5% of the expected tensile failure load at 1 Hz for 60 cycles under load-control.

.

This paper is a student paper from the 19th Injury Biomechanics Symposium and is published in a special issue of SAE International Journal of Transportation Safety.
It is preliminary work, has not been peer reviewed, and should not be cited because it is a work in progress.

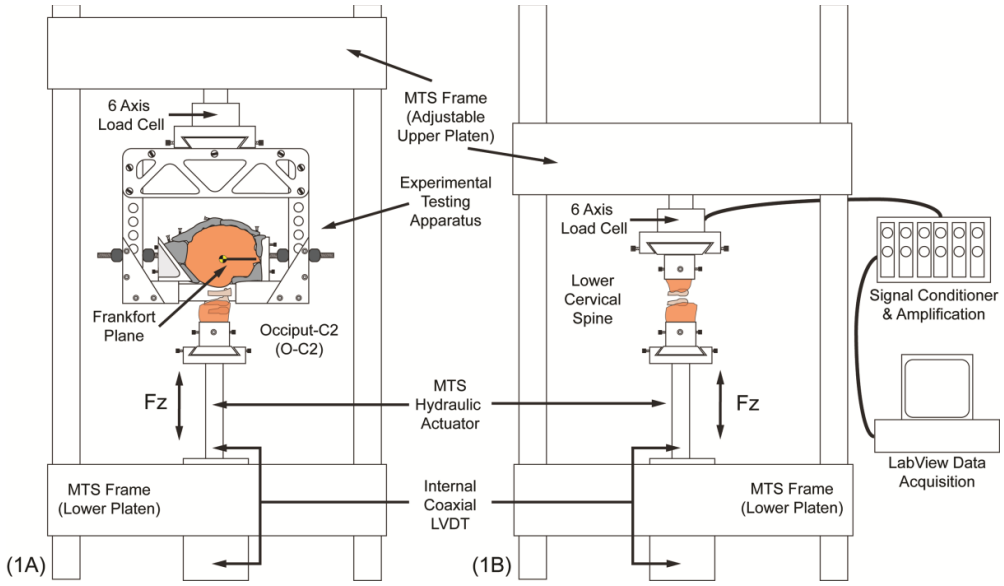

Figure 3: Pediatric motion segment tensile test setup as presented in Luck et al., 2013. 1A shows the setup of the O-C2 segment while 1B shows the setup for C4-C5 and C6-C7. All vertebrae were attached horizontally to the top and bottom plate.

Video recordings using a high-speed camera (Phantom v4.2 camera, Vision Research Inc., Wayne, NJ) of all the tests were obtained and analyzed. The sampling frequency of the camera was 100 fps, and the resolution of the images were 512 by 512 pixels under a 180 by 180mm view. The raw spatial resolution prior to post-test image tracking analysis was 0.35 mm in the sagittal plane defined by x (anteroposterior direction) and y (superior-inferior direction) axes.

Secondary Analysis

A video tracking software (TEMA Automotive, Image Systems AB, Linköping, Sweden) was used to acquire the position of each marker throughout the loading portions of both the WCS and isolated FSU (O-C2, C4-C5 and C6-C7) tests. Relevant tracking modalities for circular markers provided in TEMA—correlation, circular symmetry, and center of gravity—were examined to determine which one tracked the markers with the highest accuracy and resolution. Through trial and error, it was concluded that tracking the reflected light at the center of the balls, 1 and 2, had the highest consistency (least number of lost frames) and the highest stability. TEMA provides subpixel capabilities in tracking that is reported to be 0.01 times the pixel size, making the spatial resolution of the tests up to 0.0035mm (Kohut et al., 2015).

Throughout the entire analysis, TEMA's default 2D coordinate system was utilized. In the default coordinate system, the origin is placed at the bottom left pixel in the frame with the positive x axis pointing to the right (corresponding to the anterior direction) and the positive y axis pointing upwards (corresponding to the superior direction).

After the coordinates of each marker were obtained, the data was imported into MATLAB (R2024a, MathWorks Inc., Natick, MA) for further analysis. The tracking points were smoothed

This paper is a student paper from the 19th Injury Biomechanics Symposium and is published in a special issue of SAE International Journal of Transportation Safety.
It is preliminary work, has not been peer reviewed, and should not be cited because it is a work in progress.

using a local quadratic polynomial regression regime that spanned 15% of the data points. The coordinates, along with the beam length and assumptions (rigid insertion at a normal angle to the anterior face of the vertebral body), allow the calculation of the coordinates and orientation of the anterior vertebral body faces (further simplified as the endpoints). The coordinates of the points from the initial position at zero axial (tensile) load to peak load position (~177.6 N) were then plotted and overlayed with the initial frame and peak load frame. From those coordinates, the translation and rotation of each tracked vertebral body can be quantified in both the WCS and FSU tests and the results of such were compared and analyzed.

In the calculation of relative translation and rotation between two neighboring vertebrae, the following sign convention was utilized. A positive relative x-displacement indicates that the motion segment has extended/stretched in the x-direction, a positive relative y-displacement indicates that the motion segment exhibits a tensile response (adjacent vertebra have move away from one another), and a positive relative angle indicates that the motion segment experiences flexion. The relative magnitude is calculated by taking the square root of the square of the relative x-displacement and the relative y-displacement.

The tensile stiffnesses of the individual motion segments present in both the WCS and FSU tests (O-C2, C4-C5, and C6-C7) were then calculated and compared. The force data was acquired by downsampling the axial force data collected from the load cell to match the time and frame rate of the videos. Then, linear regression was performed on the force-displacement data from both the WCS and FSU tests to acquire the tensile stiffness. A low load (initial to ~8% peak load) and a high load (50-100% peak load) tensile stiffness were calculated to demonstrate the differences between the tensile response between the two different tests.

RESULTS

An overlay of the endpoint coordinate traces from initial position to peak load position in the WCS test is as shown in Figure 4. The difference orientation and lengths of each neighboring trace from initial position (start) to peak-load position (end) indicate that there is relative motion between each neighboring vertebra. The relative displacements in the x and y direction, the relative angles of rotation, and the relative magnitude of the displacement are summarized in Table 1.

This paper is a student paper from the 19th Injury Biomechanics Symposium and is published in a special issue of SAE International Journal of Transportation Safety.
It is preliminary work, has not been peer reviewed, and should not be cited because it is a work in progress.

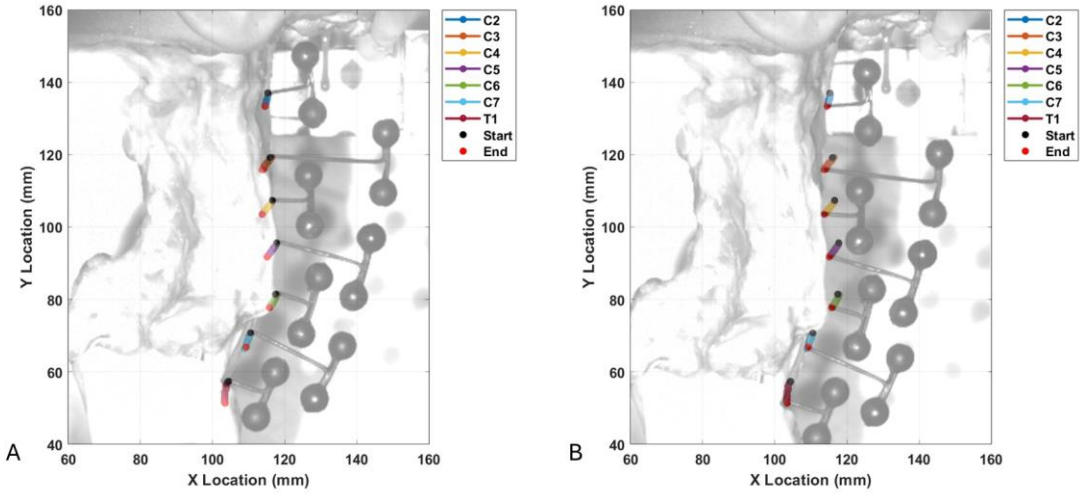

Figure 4: Coordinate traces of the anterior side of the vertebral body for C2 to T1 in the whole spine tensile test from initial position (A) to peak load position (B). From A and B, the traces of neighboring vertebra are different in terms of length and orientation, which indicates that there is relative motion between each neighboring vertebra.

This paper is a student paper from the 19th Injury Biomechanics Symposium and is published in a special issue of SAE International Journal of Transportation Safety.
It is preliminary work, has not been peer reviewed, and should not be cited because it is a work in progress.

Table 1: Relative displacement and rotation between each vertebra from initial position to peak load position in the whole cervical spine test. Sign convention is as defined in the methods.

	O – C2	**C2 – C3**	**C3 – C4**	**C4 – C5**	**C5 – C6**	**C6 – C7**	**C7 – T1**	**T1 – Plate**	**Total**
X – Displacement (mm)	-0.75	-1.75	-0.48	0.23	0.81	0.87	0.96	-0.11	-0.22
Y – Displacement (mm)	3.50	-0.17	0.33	-0.03	-0.31	0.71	1.26	0.48	5.78
Percentage of Whole Spine Y-Displacement (%)	60.6	-3.0	5.7	-0.5	-5.3	12.3	21.9	8.3	100
Angle (degrees)	-5.57	1.53	0.46	3.15	0.98	-1.26	-1.26	-1.42	0.09
Magnitude (mm)	3.58	1.76	0.58	0.23	0.87	1.12	1.59	0.49	10.23

This paper is a student paper from the 19th Injury Biomechanics Symposium and is published in a special issue of SAE International Journal of Transportation Safety.
It is preliminary work, has not been peer reviewed, and should not be cited because it is a work in progress.

Intersegmental axial displacements observed in the WCS tension tests for O-C2, C3-C4, C6-C7, and C7-T1 indicated a tensile behavior, stretching 3.50mm (60.6% of total WCS axial displacement), 0.33mm (5.74%), 0.71mm (12.3%), and 1.26mm (21.9%), respectively. C2-C3 and C5-C6 indicated a compressive response of 0.17mm (3.0%) and 0.31mm (5.3%). C4-C5 did not experience any appreciable changes in the axial direction. The total Y-displacement measured from tracking corresponds well to the LVDT peak displacement of 5.81mm with an error of 0.5%.

Furthermore, C2, C3, C4, and C5 exhibited a net flexion motion while C6 and C7 exhibited a net extension motion during WCS tensile loading. Further examination of the relative rotation between individual motion segments suggests that O-C2 had a flexion angle of 5.57 degrees and that C2-C3, C3-C4, C4-C5, and C5-C6 exhibited extension in various angles (1.53, 2.22,0.46, and 3.15, respectively) to overcome the flexion of O-C2.

The relative translation and rotation of individual motion segments present in both the WCS test and the FSU tests were compared and summarized in Table 2. Due to visible motion of the frame and head in the video of the O-C2 FSU test, the tracking results of the O-C2 test were omitted. Further analysis will be performed to subtract the effect of frame movement.

Table 2: Relative Translation and Rotation in O-C2, C4-C5, and C6-C7 in both WCS and FSU tests. The sign convention remains the same as described previously. The angles are not reported for the FSU tests as the trackers were placed on the top and bottom plates instead of the vertebra.

	O - C2 (WCS)	**O - C2 (FSU)**	**C4 - C5 (WCS)**	**C4 - C5 (FSU)**	**C6 - C7 (WCS)**	**C6 - C7 (FSU)**
X - displacement (mm)	-0.75	--	0.23	-0.040	0.87	0.032
Y- displacement (mm)	3.50	--	-0.03	0.88	0.71	1.04
Angle (degrees)	-5.57	--	0.46	--	0.98	--

Since C6-C7 exhibited a tensile response in both the WCS and FSU tests and had a relatively low angle of rotation (0.98 degrees) in the WCS test, the tensile stiffness between the WCS and FSU were compared. However, given that displacement in the x-direction was observed in the WCS condition for C6-C7, limitations exist in the comparison between the two stiffnesses and further analysis is warranted. During low-load conditions (up to around 13.5 N or ~8% of peak load), the stiffness of C6-C7 under both conditions were similar. However, at higher loads, C6-C7 became stiffer in the WCS compared to the isolated state. A linear regression of low load (0 - 8% of peak load) and high load (50 - 100% of the peak load) conditions on the loading curve was calculated and reported in Table 3.

Table 3: Stiffness of C6-C7 in the WCS and FSU under low and high loads.

	WCS	**FSU**
Low Load	68.7 N/mm	64.5 N/mm
High Load	578 N/mm	274 N/mm

This paper is a student paper from the 19th Injury Biomechanics Symposium and is published in a special issue of SAE International Journal of Transportation Safety.
It is preliminary work, has not been peer reviewed, and should not be cited because it is a work in progress.

DISCUSSION

The intersegmental kinematics of the pediatric cervical spine was measured under axial loading conditions and compared to isolated FSU tests. Intersegmental kinematics measured in the WCS tests when compared to the isolated FSU tests of the same FSUs exhibited multi-degree-of-freedom kinematics. This suggests that the tensile response of the whole cervical spine is more complex than a 1D, linear lumped-parameter model and that the numerical tensile stiffness calculated from individual FSU tests and then combined may not directly translate to whole spine stiffness. These data could be used to better understand differences in the biomechanical response of isolated FSUs when compared to their within-WCS counterparts and aid in the design of both physical and computational surrogates of the pediatric cervical spine.

The authors hypothesize that the removal of the superficial layers of the anterior and posterior longitudinal ligaments (ALL and PLL) resulted in the decrease in stiffness under high load between C6-C7 in the WCS test compared to the FSU test. This agrees with the idea that the ALL and PLL aids with cervical stabilization and support (Ivancic et al., 2007; Li-Jun et al., 2014). Furthermore, the lack of significant differences between the early loading between the WCS and FSU tests may be the result of lack of engagement and tension of these superficial layers of these intervertebral ligaments at low loads. For segments that experience more rotation, the individual elongation of the ALL and PLL needs to be considered separately as one may be in tension while the other may be lax, which will influence the overall stiffness of the motion segment.

This study is limited primarily by the small sample size. The physiological and anatomical changes in the growing pediatric cervical spine (notably ossification and stiffening of the intervertebral disc) coupled with the highly age-dependent tensile response limits the extrapolation of the results from this study to qualitative insights for the pediatric population as a whole (Kumaresan et al., 2000). Furthermore, since there is only one sample, it is difficult to quantify the accuracy of the tracking method, the validity of the assumptions associated with the trackers, and the error that is inherent within this method. However, this study does provide valuable insights into the overall intersegmental kinematics in the whole cervical spine, which with further refinement, has potential in the validation of physical and computational models of the pediatric head-neck complex based on similar age and anthropometry.

CONCLUSIONS

In this study, the tensile kinematic response of the whole cervical spine and individual motion segments of a six-year-old PMHS were quantified and compared. The presence of shear, rotation, and compressive response in the whole cervical spine indicates that bending and compressive stiffness needs to be considered within head-neck models in addition to pure tensile stiffness. In addition, the decrease in axial displacement in the C6-C7 segment suggests that longitudinal ligaments that span multiple vertebrae have an appreciable contribution to the overall axial stiffness of the neck. Extension of the study to the entire pediatric cohort tensile, flexion, and extension tests will allow the quantification of the error associated with the tracking method and

This paper is a student paper from the 19th Injury Biomechanics Symposium and is published in a special issue of SAE International Journal of Transportation Safety.
It is preliminary work, has not been peer reviewed, and should not be cited because it is a work in progress.

the development of age-dependent kinematic response and stiffness relationships between the individual motion segments and the whole cervical spine.

ACKNOWLEDGEMENTS

The authors would like to thank the members of the Duke University Injury and Orthopedic Biomechanics Laboratory, especially Jason Kait and Elizabeth Dimbath, for their technical assistance and invaluable guidance.

REFERENCES

ABELIN-GENEVOIS, K., IDJEROUIDENE, A., ROUSSOULY, P., VITAL, J. M., & GARIN, C. (2014). Cervical spine alignment in the pediatric population: A radiographic normative study of 150 asymptomatic patients. European Spine Journal, *23*(7), 1442–1448

ARAKI, T., YOKOTA, H., & MORITA, A. (2017). Pediatric Traumatic Brain Injury: Characteristic Features, Diagnosis, and Management. Neurologia medico-chirurgica, 57(2), 82–93.

ARBOGAST, K. B., BALASUBRAMANIAN, S., SEACRIST, T., MALTESE, M. R., GARCIA-ESPANA, J. F., HOPELY, T., CONSTANS, E., LOPEZ-VALDES, F. J., KENT, R. W., TANJI, H., & HIGUCHI, K. (2009). Comparison of kinematic responses of the head and spine for children and adults in low-speed frontal sled tests. SAE Technical Paper Series. https://doi.org/10.4271/2009-22-0012

CRANDALL, J. R., BOSE, D., FORMAN, J., UNTAROIU, C. D., ARREGUI-DALMASES, C., SHAW, C. G., & KERRIGAN, J. R. (2011). Human surrogates for injury biomechanics research. Clinical anatomy, 24(3), 362-371.

DIBB, A. T. (2011). Pediatric head and neck dynamic response: A computational study (Doctoral dissertation, Duke University).

DIBB, A. T., CUTCLIFFE, H. C., LUCK, J. F., COX, C. A., MYERS, B. S., BASS, C. R., ARBOGAST, K. B., SEACRIST, T., & NIGHTINGALE, R. W. (2014). Pediatric head and neck dynamics in frontal impact: Analysis of important mechanical factors and proposed neck performance corridors for 6- and 10-year-old atds. Traffic Injury Prevention, 15(4), 386–394.

This paper is a student paper from the 19th Injury Biomechanics Symposium and is published in a special issue of SAE International Journal of Transportation Safety.
It is preliminary work, has not been peer reviewed, and should not be cited because it is a work in progress.

DONG, L., LI, G., MAO, H., MAREK, S., & YANG, K. H. (2013). Development and validation of a 10-year-old child ligamentous cervical spine finite element model. Annals of biomedical engineering, 41, 2538-2552.

HAARBAUER-KRUPA, J. K., GLANG, A., KUROWSKI, B., & BREIDING, M. J. (2018). Report to congress: the management of traumatic brain injury in children.

HAIZEL-COBBINA, J., THAKKAR, R., STILL, M., SHLOBIN, N. A., IZAH, J., DU, L., SHAMIM, M. S., BONFIELD, C. M., GEPP, R., & DEWAN, M. C. (2023). Global Epidemiology of Pediatric Traumatic Spine Injury: A systematic review and meta-analysis. World Neurosurgery, 178.

IRWIN, A. L., & MERTZ, H. J. (1997). Biomechanical bases for the CRABI and Hybrid III child dummies. SAE transactions, 3551-3562.

IVANCIC, P. C., COE, M. P., NDU, A. B., TOMINAGA, Y., CARLSON, E. J., RUBIN, W., & PANJABI, M. M. (2007). Dynamic mechanical properties of intact human cervical spine ligaments. The Spine Journal, 7(6), 659-665.

KOHUT, P., KURC, K., SZYBICKI, D., CIOCH, W., & BURDZIK, R. (2015). Vision-based motion analysis and deflection measurement of a robot's crawler unit. Journal of Vibroengineering, 17(8), 4112-4121.

KUMARESAN, S., YOGANANDAN, N., PINTAR, F. A., MAIMAN, D. J., & KUPPA, S. (2000). Biomechanical study of pediatric human cervical spine: a finite element approach. J. Biomech. Eng., 122(1), 60-71.

LEONARD, J. C., BROWNE, L. R., AHMAD, F. A., SCHWARTZ, H., WALLENDORF, M., LEONARD, J. R., LERNER, E. B., & KUPPERMANN, N. (2019). Cervical spine injury risk factors in children with blunt trauma. *Pediatrics*, *144*(1).

LI-JUN, L., YING-CHAO, H., MING-JIE, Y., JIE, P., JUN, T., & DONG-SHENG, Z. (2014). Biomechanical analysis of the longitudinal ligament of upper cervical spine in maintaining atlantoaxial stability. Spinal cord, 52(5), 342-347.

LU, V. M., HERNANDEZ, N., & WANG, S. (2022). National characteristics, etiology, and inpatient outcomes of pediatric traumatic brain injury: a KID study. Child's nervous system, 38(8), 1541-1547.

LUCK, J. F., 'DALE' BASS, C. R., OWEN, S. J., & NIGHTINGALE, R. W. (2012). An apparatus for tensile and bending tests of perinatal, neonatal, pediatric and adult cadaver osteoligamentous cervical spines. Journal of Biomechanics, 45(2), 386–389.

LUCK, J. F., NIGHTINGALE, R., LOYD, A. M., PRANGE, M. T., DIBB, A. T., SONG, Y., FRONHEISER, L., & MYERS, B. S. (2008). Tensile mechanical properties of the perinatal

This paper is a student paper from the 19th Injury Biomechanics Symposium and is published in a special issue of SAE International Journal of Transportation Safety.
It is preliminary work, has not been peer reviewed, and should not be cited because it is a work in progress.

and pediatric PMHS osteoligamentous cervical spine. SAE Technical Paper, No. 2008-22-0005

LUCK, J. F., NIGHTINGALE, R. W., SONG, Y., KAIT, J. R., LOYD, A. M., MYERS, B. S., & "DALE BASS, C. R. (2013). Tensile failure properties of the perinatal, neonatal, and pediatric cadaveric cervical spine. Spine, *38*(1), E1-E12

MERTZ, H. J., IRWIN, A. L., & PRASAD, P. (2003). Biomechanical and scaling bases for frontal and side impact injury assessment reference values (No. 2003-22-0009). SAE Technical Paper.

OUYANG, J., ZHU, Q., ZHAO, W., XU, Y., CHEN, W., & ZHONG, S. (2005). Biomechanical assessment of the pediatric cervical spine under bending and tensile loading. Spine, 30(24), E716-E723.

POORMAN, G. W., SEGRETO, F. A., BEAUBRUN, B. M., JALAI, C. M., HORN, S. R., BORTZ, C. A., DIEBO, B. G., VIRA, S., BONO, O. J., DE LA GARZA-RAMOS, R., MOON, J. Y., WANG, C., HIRSCH, B. P., TISHELMAN, J. C., ZHOU, P. L., GERLING, M., & PASSIAS, P. G. (2019). Traumatic fracture of the pediatric cervical spine: Etiology, epidemiology, concurrent injuries, and an analysis of perioperative outcomes using the Kids' Inpatient Database. *International Journal of Spine Surgery*, *13*(1), 68–78.

SEACRIST, T., MATHEWS, E. A., BALASUBRAMANIAN, S., MALTESE, M. R., & ARBOGAST, K. B. (2013). Evaluation of the hybrid III and Q-series pediatric ATD upper neck loads as compared to pediatric volunteers in low-speed frontal crashes. Annals of biomedical engineering, 41, 2381-2390.

SEACRIST, T., MATHEWS, E. A., SAMUELS, M., GARCÍA-ESPAÑA, J. F., LONGHITANO, D., LAWRENCE, S. S., BALASUBRAMANIAN, S., MALTESE, M.R., & ARBOGAST, K. B. (2012, October). Kinematic comparison of the hybrid III and Q-series pediatric ATDs to pediatric volunteers in low-speed frontal crashes. In Annals of Advances in Automotive Medicine/Annual Scientific Conference (Vol. 56, p. 285). Association for the Advancement of Automotive Medicine.

SHEN, J., SHI, J., COOPER, J., CHEN, C., TAYLOR, H. G., & XIANG, H. (2021). A population-based study of the incidence, medical care, and medical expenditures for pediatric traumatic brain injury. Journal of surgical research, 268, 87-96.

SHIN, J. I., LEE, N. J., & CHO, S. K. (2016). Pediatric cervical spine and spinal cord injury: a national database study. Spine, 41(4), 283-292.

THURMAN, D. J. (2016). The epidemiology of traumatic brain injury in children and youths: a review of research since 1990. Journal of child neurology, 31(1), 20-27.

This paper is a student paper from the 19th Injury Biomechanics Symposium and is published in a special issue of SAE International Journal of Transportation Safety.
It is preliminary work, has not been peer reviewed, and should not be cited because it is a work in progress.